Neurobiology of Disease

GPR120 Signaling Controls Amyloid-*β* Degrading Activity of Matrix Metalloproteinases

Kazunori Kikuchi,[1] **Takuya Tatebe,**[1,2] **Yuki Sudo,**[1] **Miyabishara Yokoyama,**[1] **Kiwami Kidana,**[1,3] **Yung Wen Chiu,**[1] **Sho Takatori,**[1] **Makoto Arita,**[4,5] **Yukiko Hori,**[1] **and** ⬤**Taisuke Tomita**[1]

[1]Laboratory of Neuropathology and Neuroscience, Graduate School of Pharmaceutical Sciences, The University of Tokyo, Tokyo, 113-0033, Japan, [2]Faculty of Pharmaceutical Sciences, Teikyo Heisei University, Tokyo, 164-8530, Japan, [3]Department of Home Care Medicine, Graduate School of Medicine, The University of Tokyo, Tokyo, 113-0033, Japan, [4]Division of Physiological Chemistry and Metabolism, Graduate School of Pharmaceutical Sciences, Keio University, Tokyo, 105-8512, Japan, and [5]Laboratory for Metabolomics, RIKEN Center for Integrative Medical Sciences, Kanagawa, 230-0045, Japan

Alzheimer's disease (AD) is characterized by the extensive deposition of amyloid-*β* peptide (A*β*) in the brain. Brain A*β* level is regulated by a balance between A*β* production and clearance. The clearance rate of A*β* is decreased in the brains of sporadic AD patients, indicating that the dysregulation of A*β* clearance mechanisms affects the pathologic process of AD. Astrocytes are among the most abundant cells in the brain and are implicated in the clearance of brain A*β* via their regulation of the blood–brain barrier, glymphatic system, and proteolytic degradation. The cellular morphology and activity of astrocytes are modulated by several molecules, including *ω*3 polyunsaturated fatty acids, such as docosahexaenoic acid, which is one of the most abundant lipids in the brain, via the G protein-coupled receptor GPR120/FFAR4. In this study, we analyzed the role of GPR120 signaling in the A*β*-degrading activity of astrocytes. Treatment with the selective antagonist upregulated the matrix metalloproteinase (MMP) inhibitor-sensitive A*β*-degrading activity in primary astrocytes. Moreover, the inhibition of GPR120 signaling increased the levels of *Mmp2* and *Mmp14* mRNAs, and decreased the expression levels of tissue inhibitor of metalloproteinases 3 (*Timp3*) and *Timp4*, suggesting that GPR120 negatively regulates the astrocyte-derived MMP network. Finally, the intracerebral injection of GPR120-specific antagonist substantially decreased the levels of TBS-soluble A*β* in male AD model mice, and this effect was canceled by the coinjection of an MMP inhibitor. These data indicate that astrocytic GPR120 signaling negatively regulates the A*β*-degrading activity of MMPs.

Key words: Alzheimer; amyloid-beta; astrocyte; degradation; matrix metalloproteinase; protease

---

Significance Statement

The level of amyloid *β* (A*β*) in the brain is a crucial determinant of the development of Alzheimer's disease. Here we found that astrocytes, which are the most abundant cell type in the CNS, harbor degrading activity against A*β*, which is regulated by GPR120 signaling. GPR120 is involved in the inflammatory response and obesity in peripheral organs. However, the pathophysiological role of GPR120 in Alzheimer's disease remains unknown. We found that selective inhibition of GPR120 signaling in astrocytes increased the A*β*-degrading activity of matrix metalloproteases. Our results suggest that GPR120 in astrocytes is a novel therapeutic target for the development of anti-A*β* therapeutics.

Table 1. Primer sequences for qRT-PCR

Gene ID	Full name	Forward primer sequence	Reverse primer sequence
Ace	Angiotensin-converting enzyme	GAGCTGGAGAGACAAGGTGG	GTGTAGCCATTGAGCTTGGC
Apeh	Acylpeptide hydrolase	GCTCTTCCTGTATGACTGGTACAC	ACCGAGTCGAAGACCACTCT
Bsg	Basigin	CGAAGTACATAGTGGACGCAGA	CATCGGACTTGCAGACCAGT
Ctsb	Cathepsin B	CCGAACCTGCATTCACACCA	AAGCAGCCTACATGAGAATTGTAGA
Ctsd	Cathepsin D	CCTTCGCGATTATCAGAATCCCTC	ACGACTGTGAAACACTGCGG
Gpr120	Gpr120	TTGTGACTTTGAACTTCCTGGTG	GTATGCCAAGCTCAGCGTAAG
Gapdh	Glyceraldehyde 3-phosphate dehydrogenase	AGGTCGGTGTGAACGGATTTG	TGTAGACCATGTAGTTGAGGTCA
Ide	Insulin-degrading enzyme	CCACGAGGCTATACGTCCAA	AAACTATTGCCACCCGCACA
Klk7	Kallikrein-related peptidase 7	ACTCCACAAAGACCCACGTC	CGAGGGAAAGGTCACGTCTG
Mbp	Myelin basic protein	GGCATCCTTGACTCCATCGG	TCCTTGTACATGTGGCACAGC
Mme	Membrane metallo-endopeptidase	AACTTTGCCCAGGTGTGGTG	AAAGGCATCTGCAAACTCGG
Mmel1	Membrane metalloendopeptidase-like 1	CCACCGAATGGACCTGATGG	GCATGGTCCGTGCTGAGTAG
Mmp14	MMP 14	CCAAGGCAGCAACTTCAGC	GTGAGCGTTGTGTGTGGGTA
Mmp2	MMP 2	CAAGTTCCCCGGCGATGTC	TTCTGGTCAAGGTCACCTGTC
Mmp9	MMP 9	GCGTCATTCGCGTGGATAAG	CCTGGTTCACCTCATGGTCC
Plat	Tissue-type plasminogen activator	AGCGAGGACTGCTATGTTGG	TCACCATCTGGATTCCGACAA
Plg	Plasminogen	CAGATTCCTCAGTTCCACCAGA	AGTTCATCTCCAAGCCAGCA
Timp1	TIMPs 1	AGACACACCAGAGCAGATACC	TGGTATAAGGTGGTCTCGTTGATT
Timp2	TIMPs 2	AGTGCAAGATCACTCGCTGT	CGCGCAAGAACCATCACTTC
Timp3	TIMPs 3	TGCCTTCTGCAACTCCGAC	TGAAGCCTCGGTACATCTTCATC
Timp4	TIMPs 4	TTGACTGGCCAGATTCTCAGT	GCACTGCATAGCAAGTGGTG
Ace	Angiotensin-converting enzyme	GAGCTGGAGAGACAAGGTGG	GTGTAGCCATTGAGCTTGGC
Apeh	Acylpeptide hydrolase	GCTCTTCCTGTATGACTGGTACAC	ACCGAGTCGAAGACCACTCT
Bsg	Basigin	CGAAGTACATAGTGGACGCAGA	CATCGGACTTGCAGACCAGT
Ctsb	Cathepsin B	CCGAACCTGCATTCACACCA	AAGCAGCCTACATGAGAATTGTAGA
Ctsd	Cathepsin D	CCTTCGCGATTATCAGAATCCCTC	ACGACTGTGAAACACTGCGG
Gpr120	Gpr120	TTGTGACTTTGAACTTCCTGGTG	GTATGCCAAGCTCAGCGTAAG
Gapdh	Glyceraldehyde 3-phosphate dehydrogenase	AGGTCGGTGTGAACGGATTTG	TGTAGACCATGTAGTTGAGGTCA
Ide	Insulin-degrading enzyme	CCACGAGGCTATACGTCCAA	AAACTATTGCCACCCGCACA
Klk7	Kallikrein-related peptidase 7	ACTCCACAAAGACCCACGTC	CGAGGGAAAGGTCACGTCTG
Mbp	Myelin basic protein	GGCATCCTTGACTCCATCGG	TCCTTGTACATGTGGCACAGC
Mme	Membrane metallo-endopeptidase	AACTTTGCCCAGGTGTGGTG	AAAGGCATCTGCAAACTCGG
Mmel1	Membrane metalloendopeptidase-like 1	CCACCGAATGGACCTGATGG	GCATGGTCCGTGCTGAGTAG
Mmp14	MMP 14	CCAAGGCAGCAACTTCAGC	GTGAGCGTTGTGTGTGGGTA
Mmp2	MMP 2	CAAGTTCCCCGGCGATGTC	TTCTGGTCAAGGTCACCTGTC
Mmp9	MMP 9	GCGTCATTCGCGTGGATAAG	CCTGGTTCACCTCATGGTCC
Plat	Tissue-type plasminogen activator	AGCGAGGACTGCTATGTTGG	TCACCATCTGGATTCCGACAA
Plg	Plasminogen	CAGATTCCTCAGTTCCACCAGA	AGTTCATCTCCAAGCCAGCA
Timp1	TIMPs 1	AGACACACCAGAGCAGATACC	TGGTATAAGGTGGTCTCGTTGATT
Timp2	TIMPs 2	AGTGCAAGATCACTCGCTGT	CGCGCAAGAACCATCACTTC
Timp3	TIMPs 3	TGCCTTCTGCAACTCCGAC	TGAAGCCTCGGTACATCTTCATC
Timp4	TIMPs 4	TTGACTGGCCAGATTCTCAGT	GCACTGCATAGCAAGTGGTG

Introduction

Alzheimer's disease (AD) is the most common neurodegenerative disorder among the dementias. It is characterized by the extensive deposition of amyloid-β peptide (Aβ) as senile plaques in the brain. Aβ is mainly secreted from neuronal cells by the proteolytic processing of amyloid precursor protein (APP). This processing is performed sequentially by β-site APP cleaving enzyme 1 (BACE1) and γ-secretase. Genetic analyses demonstrated that many autosomal-dominant AD mutations augment Aβ production or aggregation (Kikuchi et al., 2017; Tomita, 2017), and the point mutation encoding for A673T in Aβ sequence protects against AD and cognitive decline in older people without AD (Jonsson et al., 2012). In sporadic patients, whereas Aβ production was found to be unaltered, the clearance rate of brain Aβ was significantly decreased (Mawuenyega et al., 2010). Thus, the dysregulation of Aβ clearance affects brain Aβ level, the deposition of senile plaques, and the pathologic process of AD. Recently, the pathophysiological contribution of astrocytes in Aβ clearance has been highlighted. Astrocytes modulate the blood–brain barrier, phagocytic activity, the glymphatic system, and activities of Aβ-degrading enzymes (Saido and Leissring, 2012; Ries and Sastre, 2016). However, the precise regulatory mechanism of Aβ-degrading enzymes remains unclear.

The brain is a lipid-enriched organ in the body. Lipids account for about half of the dry weight of the brain (O'Brien and Sampson, 1965; Liu et al., 2015), and include polyunsaturated fatty acids (PUFAs). PUFAs are mostly esterified and exist in the cellular membrane, and are partially released from the membrane by the activity of phospholipases. These unesterified PUFAs and their metabolites function as lipid mediators, and transduce various cellular signaling pathways via their cognate receptors (Ishihara et al., 2019). Epidemiological studies have shown that a high consumption of ω3 PUFAs, such as docosahexaenoic acids (DHA), is associated with a reduced risk of AD (Morris et al., 2003). Many studies also suggested the multifunctional beneficial effects of ω3 PUFAs on AD (Bazinet and Layé, 2014). DHA in the cellular membrane prevents Aβ-induced neuronal apoptosis by activation of the extracellular signal-

regulated kinase (ERK) pathway (Florent et al., 2006; Kim et al., 2010). Additionally, neuroprotectin D1, a lipid mediator derived from DHA (Schwab et al., 2007), suppressed Aβ production via peroxisome proliferator-activated receptor γ (Zhao et al., 2011). Other reports suggested that DHA induces the differentiation, inflammatory response, and morphologic changes of astrocytes (Heras-Sandoval et al., 2016; Das and Das, 2019; Yu et al., 2020). However, the effects of ω3 PUFAs on the Aβ-degrading activity of astrocytes are not well characterized.

ω3 PUFAs activate the GPCR GPR120/FFAR4 (Hirasawa et al., 2005; Oh and Olefsky, 2016). GPR120 is widely expressed in various tissues, including the gastrointestinal tract, adipose tissue, and brain. GPR120 signaling facilitates the activities of glucagon-like peptide-1 in the gut (Hirasawa et al., 2005), promotes adipogenesis in adipose tissue (Gotoh et al., 2007; Hilgendorf et al., 2019), and suppresses the activation of the macrophages induced inflammatory response (Oh et al., 2010). Thus, the therapeutic potential of GPR120 has focused on Type 2 diabetes (Oh and Olefsky, 2016; Milligan et al., 2017). Moreover, recent studies showed that GPR120 is expressed in astrocytes, microglia, and neuronal cells (Ren et al., 2019), and DHA treatment regulates the morphology of astrocytes via GPR120 signaling (Das and Das, 2019). However, the association between GPR120 and Aβ clearance by astrocytes remains unclear. Therefore, in this study, we analyzed the mechanism by which GPR120 signaling regulates the Aβ-degrading activity of astrocytes.

Materials and Methods

Cell culture and compounds. All cells used in this report were cultured in DMEM with high glucose (Wako) containing 10% heat-inactivated FBS (Hyclone), 50 unit/ml penicillin (Wako), and 50 units/ml streptomycin (Wako) at 37°C in humidified 5% CO_2 air (Tomita et al., 1997; Kidana et al., 2018). Primary glial cells, mainly comprised of astrocytes, were obtained as previously described with some modifications (Fukumoto et al., 1999; Kidana et al., 2018). Briefly, we isolated cerebrum from postnatal day 2 mice of either sex in ice-cold HBSS(−) (Wako). The cerebrum was suspended in HBSS containing 0.25% trypsin, 0.1 μl/ml DNase (Nippon Gene), 0.8 mM $MgSO_4$ (Kanto), and 1.85 mM $CaCl_2$ (Kanto) at 37°C for 15 min. The obtained cell suspension was passed through a 100 μm cell strainer (Falcon) and centrifuged with culture medium. The cell pellet was resuspended in culture medium and seeded on cell culture plate. The culture medium was renewed at 4 DIV and thereafter every 2-3 d. 7PA2 cell (Podlisny et al., 1995), a cell line obtained by transfecting human APP751 with V717F mutation to Chinese hamster ovary cells, was kindly provided by Dr. Edward Koo (University of California, San Diego). The conditioned medium (CM) of 7PA2 cells (7PA2 CM) cultured at confluency for 2 d was collected and centrifuged at $6000 \times g$ for 10 min at 4°C to remove cell debris. Then, Aβ40 level in 7PA2 CM was determined by ELISA (Human/Rat β Amyloid(40) ELISA Kit Wako II, Wako, catalog #294-64701). Cell viability was checked by using alamarBlue Cell Viability Reagent (Thermo Fisher Scientific, catalog #DAL1025). Docosahexaenoic acid (Cayman Chemical, catalog #90310), compound A (Cayman Chemical, catalog #16624), AH7614 (Focus Biomolecules, catalog #10-1521), and GM6001 (Enzo Life Science, catalog #BML-EI300-0005) were purchased from the indicated suppliers.

Immunologic methods. Samples were dissolved in Laemmi sample buffer (final concentration: 2% SDS, 80 mM Tris-HCl pH 6.8, 10% glycerol, 0.0025% Brilliant green [Wako], 0.00625% Coomassie Brilliant Blue G250 [Nacalai Tesque]) and boiled for 5 min at 100°C. For detection of membrane proteins in 2% Triton X-100-soluble fraction extracted from mouse hippocampus, samples were incubated 5 min at 65°C instead of boiling. Western blotting was performed as described previously (Tomita et al., 1997; Kidana et al.,

2018). Aβ40 and Aβ42 derived from 7PA2 CM were detected by SDS-PAGE using acrylamide gel containing 8 M urea (urea/SDS-PAGE), as described previously (Qi-Takahara et al., 2005; Ohki et al., 2011). For assessment of immunoreactivity, chemical fluorescence of ImmunoStar detection kit (Wako, catalog #291-55203) or Supersignal West Femto (Pierce, catalog #34096) was detected by Image Quant LAS 4000 (GE Healthcare). Signal intensity was quantified by ImageQuant TL software (GE Healthcare). For Aβ-degrading assay, DIV12-DIV14 primary astrocytes were treated 20 nM synthetic human Aβ40 (Peptide Institute, catalog #4307-v) or 7PA2 CM (final Aβ40 concentration: 2 nM) with compounds (Kidana et al., 2018). After indicated times, levels of remaining Aβ were analyzed by Western blotting. The antibodies for the Western blotting were the following: anti-human Aβ (82E1, IBL, catalog #10323, 1:2500 dilution), anti-α-tubulin (DM1A, Sigma Millipore, catalog #T9026, 1:5000 dilution), anti-human sAPPβ-sw (6A1, IBL, catalog #10321, 1:200), anti-BACE1 (BACE1(c), Wako, catalog #18711, 1:1000 dilution), and anti-Na$^+$/K$^+$-ATPase (a6F, DSHB, RRID: AB_528092, 1:1000 dilution).

qRT-PCR. Total RNA was extracted from cells using Isogen (Nippon Gene, catalog #311-02501). Then, cDNA synthesis from total RNA was performed using ReverTra Ace qPCR RT Master Mix with gDNA Remover (Toyobo, catalog #FSQ-301) according to the supplier's instruction. cDNA mixed with gene-specific primers and Thunderbird SYBR qPCR Mix (Toyobo, catalog #QPS-201), and qRT-PCR was run on LightCycler 480 Instrument (Roche). The PCR condition was as follows: 1 cycle of denaturation (95°C, 1 min); 50 cycles of denaturation (95°C, 10 s), annealing (60°C, 30 s), and extension (72°C, 1 min). Specificity was confirmed by melting curve analysis and agarose gel electrophoresis. The sequences of primers used qRT-PCR are listed in Table 1.

Preparation of lentiviral short hairpin RNA. pLKO.1-puro vector (a gift from Bob Weinberg, Addgene plasmid #8453; http://n2t.net/addgene:8453; RRID:Addgene_8453) is lentiviral vector for small interfering RNA expression encoding puromycin resistance gene under the human phosphoglycerate kinase promoter (Stewart et al., 2003). We removed the puromycin resistance gene from this vector and inserted EGFP gene to construct the pLKO.1-EGFP vector (Chiu et al., 2020). Short hairpin RNA (shRNA) sequences were cloned into pLKO.1-EGFP according to the protocol by Addgene. The sequences of primers used for plasmid construction are listed in Table 2. Two different shRNA sequences (#1 and #2) were designed for each gene, based on GPP Web Portal site (https://portals.broadinstitute.org/gpp/public/) and Invitrogen BLOCK-iT RNAi Designer

Table 2. The sequences of primers for lentiviral shRNA constructs

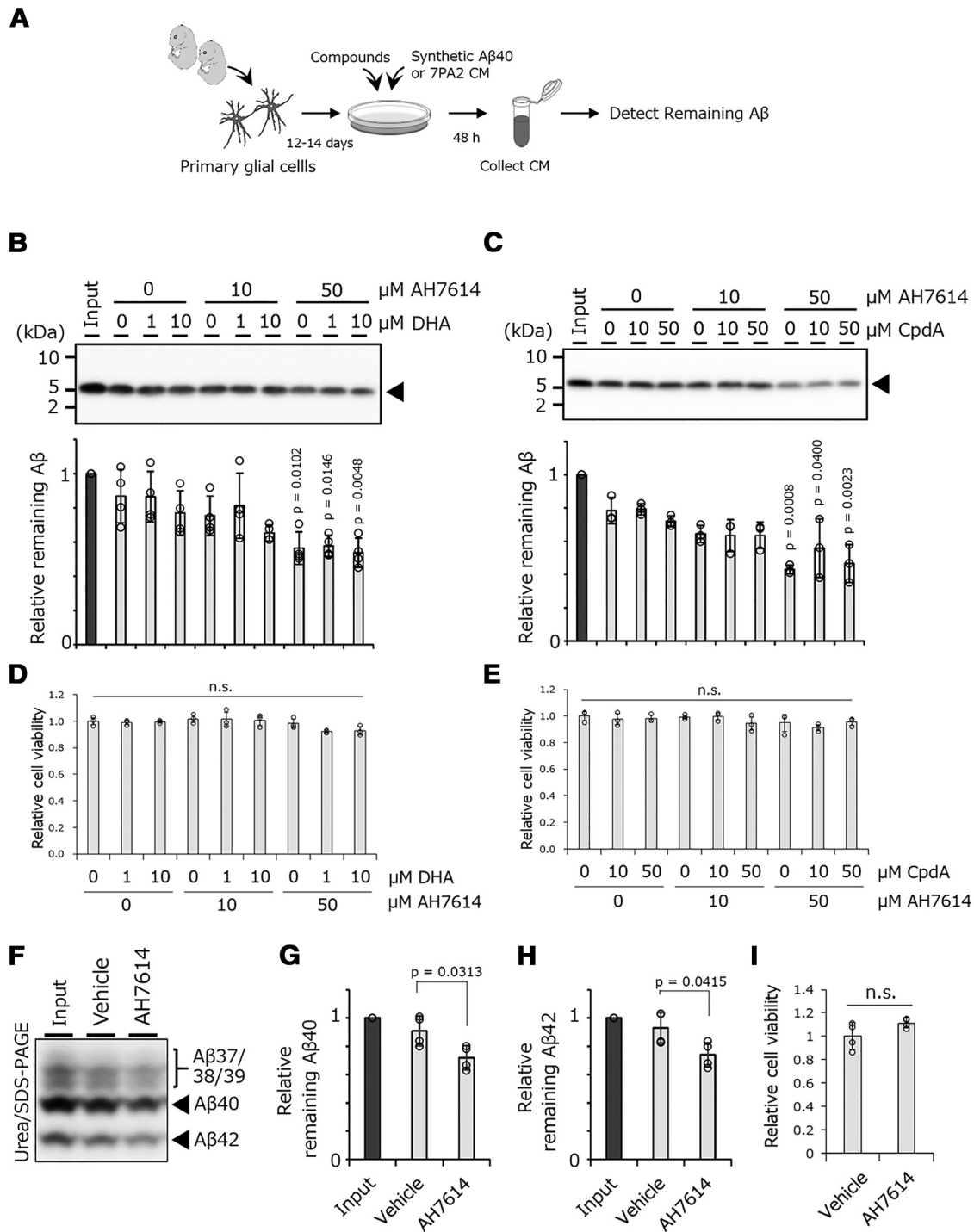| shRNAs	Primer sequence[a]
shLuci	CCGGCTTACGCTGAGTACTTCGACTCGAGTCGAAGTACTCAGCGTAAGTTTTTG
	AATTCAAAAACTTACGCTGAGTACTTCGACTCGAGTCGAAGTACTCAGCGTAAG
shGpr120 #1	CCGGCGAAATGACTTGTCTGTTATTCTCGAGAATAACAGACAAGTCATTTCGTTTTTG
	AATTCAAAAACGAAATGACTTGTCTGTTATTCTCGAGAATAACAGACAAGTCATTTCG
shGpr120 #2	CCGGCCCAACCGCATAGGAGAAATCTCATCTCGAGATGAGATTTCTCCTATGCGGTT
	GGGTTTTTG
	AATTCAAAAACCCAACCGCATAGGAGAAATCTCATCTCGAGATGAGATTTCTCCTA
	TGCGGTTGGG
shMmp2 #1	CCGGGCTGAAAGATACCCTCAAGAACTCGAGTTCTTGAGGGTATCTTTCAGCTTTTTG
	AATTCAAAAAGCTGAAAGATACCCTCAAGAACTCGAGTTCTTGAGGGTATCTTTCAGC
shMmp2 #2	CCGGGCTGTGTTCTTCGCAGGGAATCTCGAGATTCCCTGCGAAGAACACAGCTTTTTG
	AATTCAAAAAGCTGTGTTCTTCGCAGGGAATCTCGAGATTCCCTGCGAAGAACACAGC
shMmp9 #1	CCGGGAGGCATACTTGTACCGCTATCTCGAGATAGCGGTACAAGTATGCCTCTTTTTG
	AATTCAAAAAGAGGCATACTTGTACCGCTATCTCGAGATAGCGGTACAAGTATGCCTC
shMmp9 #2	CCGGCCACTTACTATGGAAACTCAACTCGAGTTGAGTTTCCATAGTAAGTGGTTTTTG
	AATTCAAAAACCACTTACTATGGAAACTCAACTCGAGTTGAGTTTCCATAGTAAGTGG
shMmp9 #1	CCGGGCAGTGATGAAGTCTTCCACATCTCGAGATGTGAAGACTTCATCACTGCTTTTTG
	AATTCAAAAAGCAGTGATGAAGTCTTCCACATCTCGAGATGTGAAGACTTCATCACTGC
shMmp9 #2	CCGGCCATCAATACTGCCTACGAAACTCGAGTTTCGTAGGCAGTATTGATGGTTTTTG
	AATTCAAAAACCATCAATACTGCCTACGAAACTCGAGTTTCGTAGGCAGTATTGATGG

[a]Upper, forward primer; lower, reverse primer.

Figure 1. AH7614 treatment induced Aβ-degrading activity in primary astrocytes. **A**, Schematic depiction of the Aβ-degrading assay. DIV12 to DIV14 primary astrocytes were treated with compounds and Aβ (synthetic Aβ40 or 7PA2 CM) for 48 h. Then, the level of remaining Aβ in the mixture was analyzed by Western blotting. **B**, Degradation of synthetic Aβ40 by primary astrocytes treated with DHA and with or without AH7614. A representative Western blot and quantified results are shown ($n = 4$, mean $\pm$ SD, Dunnett test vs 0 μM DHA). **C**, Degradation of synthetic Aβ40 by primary astrocytes treated with CpdA, with or without AH7614. Representative Western blot and quantified results are shown ($n = 3$, mean $\pm$ SD, Dunnett test vs 0 μM CpdA). **D**, The cell viability was measured by using alamarBlue under the condition in **C** ($n = 3$, mean $\pm$ SD, Dunnett test vs 0 μM DHA). **E**, The cell viability was measured by using alamarBlue under the condition in **C** ($n = 3$, mean $\pm$ SD, Dunnett test vs 0 μM CpdA). **F**, Representative Western blot of the remaining level of 7PA2 CM-derived Aβ species after incubation with CM of primary astrocytes treated with AH7614. **G**, Quantified results of the remaining Aβ40 from 7PA2 cells ($n = 4$, mean $\pm$ SD, Student t test vs the Vehicle group). **H**, Quantified results of the remaining Aβ42 from 7PA2 cells ($n = 4$, mean $\pm$ SD, Student t test vs the Vehicle group). **I**, The cell viability was measured by using alamarBlue under the condition in **F-H** ($n = 4$, mean $\pm$ SD, Student t test vs the Vehicle group).

(https://rnaidesigner.thermofisher.com/rnaiexpress/). The sequence of control shRNA targeting luciferase (shLuci) was designed with reference to the previous report (Lewis et al., 2002). For production of recombinant lentiviral particle, LentiX-293T cells (Takara Bio)

were transiently transfected packaging plasmids (pCAG-KGP4.1R, pCAG4-RTR2, and pCAGS-VSVG; a gift from Dr. Haruhiko Bito, The University of Tokyo) with pLKO.1-EGFP containing shRNA sequences using PEI (Okuno et al., 2012; Miyagawa et al., 2016;
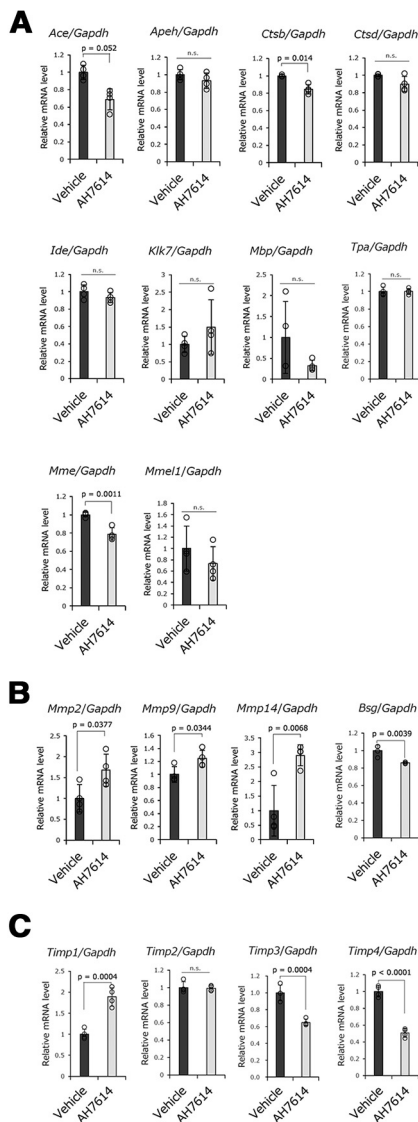
Figure 2. AH7614 treatment affected the expression levels of Aβ-degrading enzymes and associated factors. The mRNA expression levels of known Aβ-degrading enzymes and their activators (**A,B**) and TIMPs (**C**) in primary astrocytes treated with 50 μM AH7614 and 7PA2 CM for 24 h were quantified by qRT-PCR (n = 4, mean ± SD, Student t test vs the Vehicle group). The mRNA expression of *Plau* encoding plasminogen, *Klk5* encoding kallikrein-related peptidase 5, and *Spink5* encoding endogenous inhibitor for KLKs was undetectable in primary astrocytes.

Chiu et al., 2020). After 6 h, medium was refreshed. Thereafter, medium was collected and refreshed daily for 2 d. The lentiviral particle in medium was concentrated using Lenti-X concentrator (Takara Bio, catalog #631231) and resuspended in DMEM. For knockdown in primary astrocytes, the lentiviral particles were infected at DIV5. Two days after infection, the medium was changed, and the infected cells were cultured for the indicated period.

Animals. All experiments using animals were performed according to the guidelines provided by the Institutional Animal Care Committee of Graduate School of Pharmaceutical Sciences, The University of Tokyo (Protocol P29-30 and P30-3). APP/PS1 mice (B6.Cg-Tg(APPswe, PSEN1dE9)85Dbo/Mmjax, The Jackson Laboratory, JAX mouse #005864) express a chimeric mouse/human APP with the Swedish mutation (K670M/K671L) and human PSEN1 gene with exon 9 deletion under the murine prion promoter (Jankowsky et al., 2004).

Injection of compounds into mice hippocampi. Injection of compounds into mouse hippocampus was performed as described

previously (Hori et al., 2015; Kidana et al., 2018). Briefly, 4 μl of 100 μM AH7614 and 2% DMSO (vehicle) in PBS, respectively, was injected at 0.3 μl/min into the right and left hippocampus (AP: −2.0 mm from bregma, ML: ±1.5 mm from midline, DV: −1.7 mm below brain surface) in 12- to 15-month-old male APP/PS1 mice (n = 7). Twenty-four hours after injection, injected sides of hippocampi were collected from these mice. The change of protein level by AH7614 injection was compared between the left and right hippocampi of individual mice.

Brain extraction and fractionation. Mice hippocampi were homogenized in extraction buffer and centrifuged at 246,200 × g for 20 min (stepwise). The extraction buffers for each step were the following: first step: TBS, 0.05 M Tris, 0.15 M NaCl, 0.02 tab/ml cOmplete (Roche), 0.1 tab/ml PhosSTOP (Roche), adjusted pH 7.6 by HCl); second step: 2% Triton X-100 in TBS; third step: 2% SDS in TBS. The 2% SDS-insoluble fraction was sonicated in 70% formic acid and centrifuged at 246,200 × g for 20 min. Then, the resultant supernatant was freeze-dried for 2 h using Savant RVT5105 (Thermo Fisher Scientific). The pellet was dissolved in DMSO. Protein concentration of each fraction was determined by BCA protein assay (Thermo Fisher Scientific).

Data availability. Two public RNAseq datasets were obtained from AMP-AD Knowledge Portal (https://www.synapse.org/#!Synapse: syn2580853) as previously described (Allen et al., 2016; Wang et al., 2018): the Mayo sample set and Mount Sinai Brain Bank (MSBB) studies. The Mayo study comprises temporal cortex samples from 164 subjects with the following pathologic diagnosis: 84 patients with AD and 80 controls. We assessed the expression levels of tissue inhibitor of the metalloproteinases 3 (TIMP3), TIMP4, matrix metalloproteinase 2 (MMP2), MMP9, MMP14, and FFAR4 in the temporal cortex between AD patients and controls by a simple model (syn6090804) adjusting for key covariates: age at death, gender, RNA integrity number (RIN), source, and flow cell. For the MSBB study, we obtained clinical information of each subject, RNAseq covariates, and normalized RNA read counts of above targets (syn7391833). As described in the previous report (syn20801188), gene level expression (read counts) was corrected for known covariates factors, including postmortem interval, race, batch, sex, RIN, and exonic rate to remove the confounding effects. The trimmed mean of M values normalization method was used to estimate scaling factors and adjust for differences in library sizes. We selected 201 samples of the parahippocampal gyrus (Brodmann area 36) from subjects and excluded the samples without the information of the Braak NFT stage. These data were applied and analyzed using Python Jupyter Notebook. The comparison of expression levels of TIMP3, TIMP4, MMP2, MMP9, MMP14, and FFAR4 was performed among different categories described as follows: We divided samples into two categories, healthy control subjects and AD patients, depending on the NP.1 stage, neuropathology category as measured by CERAD.

Statistical analysis. Data are presented as mean values, and error bars indicate SD. For data analysis, paired t test, Student's t test, Tukey test, and Dunnett test were performed using KyPlot (KyensLab) or Excel (Microsoft) software. For analysis of RNAseq datasets, Mann–Whitney U test, Kruskal–Wallis test with Dunn's *post hoc* analysis, and Kendall rank correlation were performed to compare the gene expression levels. A p value < 0.05 was considered to have a significant difference.

Result

Treatment of GPR120-selective antagonist upregulated the Aβ-degrading activity of primary astrocytes

GPR120 is abundantly expressed in the gastrointestinal tract (Hirasawa et al., 2005). Recent analyses demonstrated that GPR120 is also expressed in the brain (Dragano et al., 2017; Ren et al., 2019). We also confirmed the expression of endogenous GPR120 in primary glial cells, mainly comprised of astrocytes (see below in Fig. 3D). To investigate whether GPR120 signaling affects the Aβ-degrading activity of astrocytes, we analyzed the effects of DHA, the GPR120-
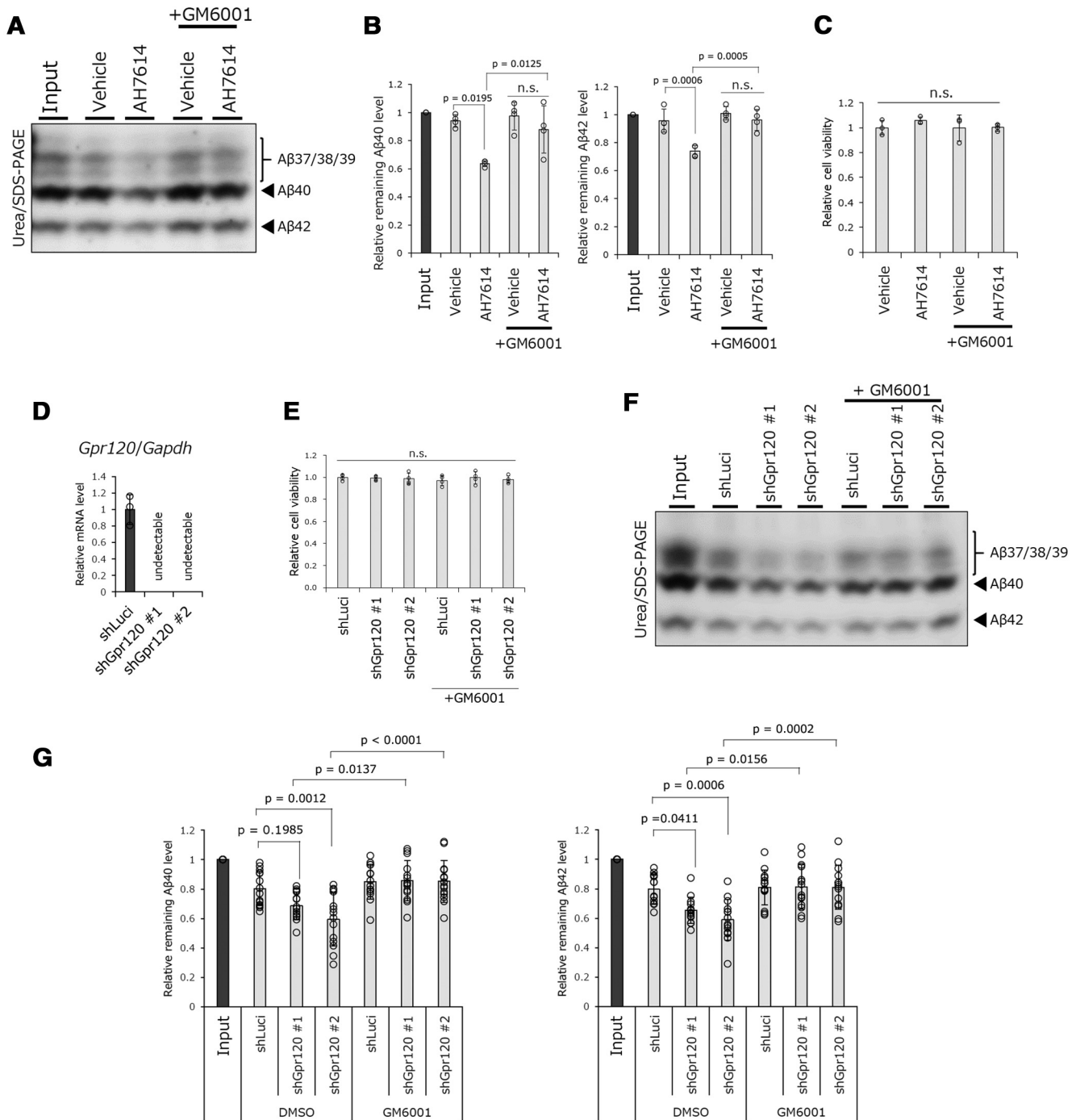
Figure 3. GM6001 treatment abolished the Aβ-degrading activity induced by suppression of GPR120 signaling. ***A***, Representative Western blot of the remaining levels of 7PA2 CM-derived Aβ40 and Aβ42 in the mixture of CM from primary astrocytes treated with 50 μM AH7614 with or without 25 μM GM6001 for 48 h. ***B***, Quantified results of the remaining Aβ40 and Aβ42 in ***A*** ($n = 4$, mean ± SD, Tukey test). ***C***, The cell viability was measured by using alamarBlue under the condition in ***A***, ***B*** ($n = 3$, mean ± SD, Tukey test). ***D***, Seven days after infection of lentiviral shRNAs for luciferase (shLuci) or two different target sequences in Gpr120 (shGpr120 #1 or #2), Gpr120 expression levels in primary astrocytes were quantified by qRT-PCR ($n = 3$, mean ± SD, Dunnett test vs the shLuci group). ***E***, The cell viability was measured by using alamarBlue under the condition in ***F***, ***G*** ($n = 4$, mean ± SD, Tukey test). ***F***, At DIV12, Gpr120-knockdown primary astrocytes were treated with 7PA2 CM and with or without 25 μM GM6001. After 96 h, the remaining level of 7PA2 CM-derived Aβ40 and Aβ42 in CM was quantified by Western blotting. ***G***, Quantified results of ***F*** ($n = 14$, mean ± SD, Tukey test).

selective agonist compound A (CpdA) (Oh et al., 2014), and the GPR120-selective antagonist AH7614 (Sparks et al., 2014; Watterson et al., 2017) on the Aβ-degrading assay using synthetic human Aβ40 (Kidana et al., 2018) (Fig. 1A). Although treatment with DHA or CpdA showed no effects, treatment with AH7614 significantly decreased the levels of remaining Aβ in the CM (Fig. 1B,C) without affecting the cell viability (Fig. 1D,E). Moreover,

AH7614 treatment significantly enhanced the degrading activity of astrocytes for various Aβ species in the CM of 7PA2 cells, which stably express mutant human APP and secrete a robust amount of several Aβ species (Podlisny et al., 1995) (Fig. 1F–I). These results suggested that the inhibition of GPR120 in astrocytes upregulated the degrading activity of not only synthetic Aβ, but also naive Aβ species secreted from the cultured cells.
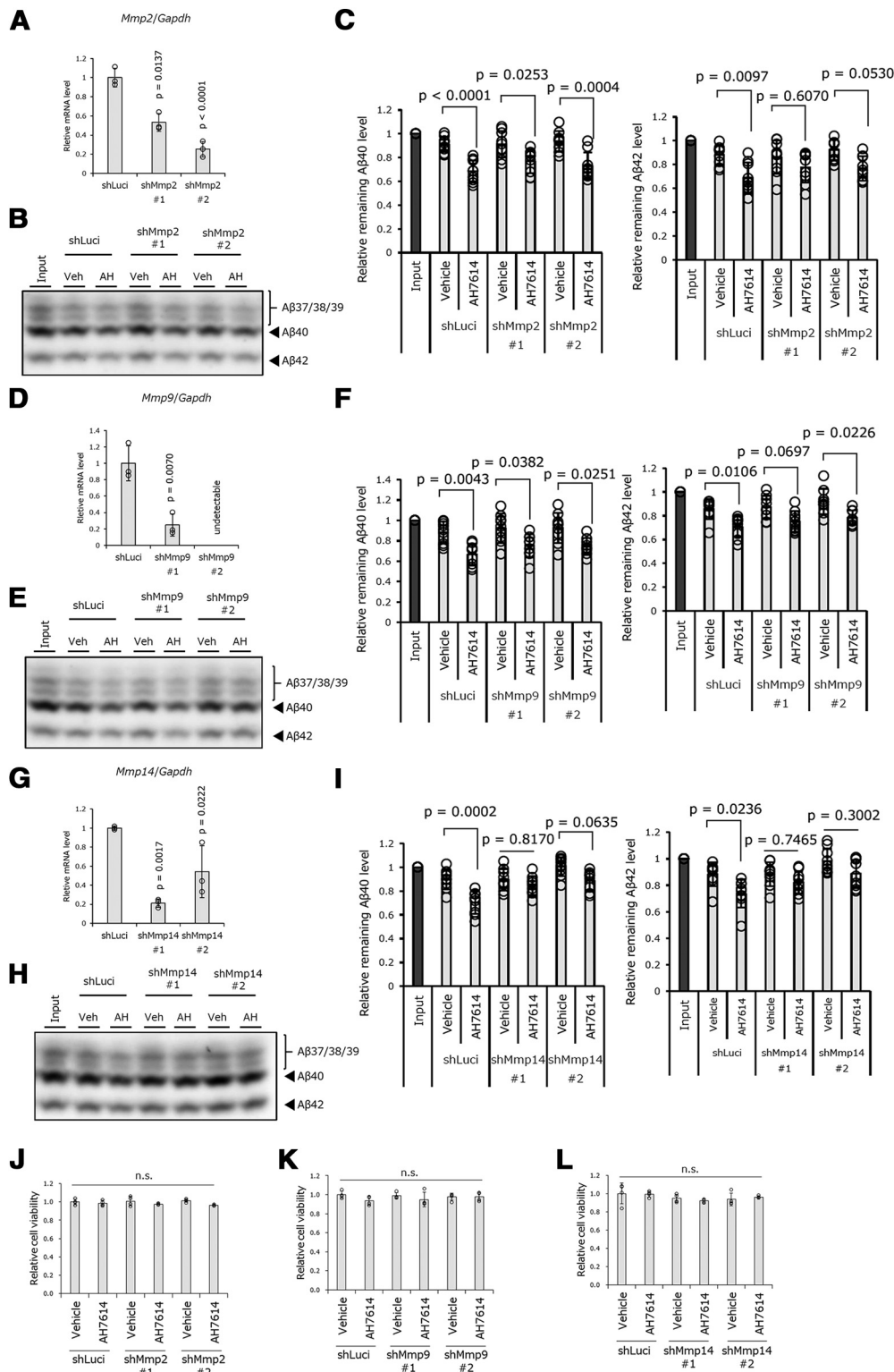
Figure 4. *MMP14* knockdown, but neither *MMP2* nor *MMP9* knockdown, suppressed the Aβ-degrading activity induced by AH7614 treatment. Seven days after infection of lentiviral shRNAs targeting luciferase, *Mmp2* (**A-C**), *Mmp9* (**D-F**), and *Mmp14* (**G-I**) into primary astrocytes, mRNA expression levels were quantified by qRT-PCR ($n = 3$, mean ± SD, Dunnett test vs shLuci group) (**A,D,G**). At DIV12, the infected primary astrocytes were treated with 7PA2 CM and with 50 μM AH7614 for 48 h. Then, the remaining levels of 7PA2 CM-derived Aβ40 and Aβ42 in the CM of each sample were analyzed by Western blotting (**B,E,H**). **C, F, I**, Quantified results ($n = 9$, mean ± SD, Tukey test). The cell viability was measured by using alamarBlue under the condition in **B, C** (**J**, $n = 4$, mean ± SD, Tukey test), in **E, F** (**K**, $n = 4$, mean ± SD, Tukey test), and in **H, I** (**L**, $n = 4$, mean ± SD, Tukey test).

GPR120 regulated the Aβ-degrading activity regulated by MMP14

Next, we analyzed the expression levels of mRNAs of known degrading enzymes for extracellular Aβ in AH7614-treated primary astrocytes (Saido and Leissring, 2012; Ries and Sastre, 2016; Kidana et al., 2018). No change was observed in the expression level of *Apeh* (Yamin et al., 2007), *Ctsd* (Hamazaki, 1996; McDermott and Gibson, 1996), *Ide* (Qiu et al., 1998), *Klk7*

Table 3. Mayo RNAseq cohort shows the changes in *FFAR4*, *MMP2*, *MMP9*, *MMP14*, *TIMP3*, and *TIMP4* mRNA levels in AD patients[a]

Gene name	Dx β	Effect direction	Dx q
FFAR4	−1.175087753	Down in AD	3.12E-06
MMP2	0.393271813	Up in AD	0.060226773 (ns)
MMP9	0.93970622	Up in AD	0.004726111
MMP14	0.836293303	Up in AD	0.000186216
TIMP3	0.900172204	Up in AD	3.66E-06
TIMP4	0.261013671	Up in AD	0.227104156 (ns)

[a]Comparison of the *FFAR4*, *MMP2*, *MMP9*, *MMP14*, *TIMP3*, and *TIMP4* mRNA levels from 80 control and 84 AD subjects. Normalized read counts of mRNAs were assessed by the simple model considering the factors, including age at death, gender, RIN, source, and flow cell. Dx β indicates the regression coefficient. Effect direction indicates the changes in target mRNA level between control and AD patients. Dx q indicates the adjusted p value with a significant difference when Dx $q < 0.05$.

(Kidana et al., 2018), *Mbp* (Liao et al., 2009), *Mmel1* (Shirotani et al., 2001), or *Tpa* (Van Nostrand and Porter, 1999) mRNA (Fig. 2A). In addition, levels of *Ace* (Hu et al., 2001) and *Mme* (Shirotani et al., 2001) mRNAs were significantly decreased (Fig. 2A). In contrast, AH7614 treatment increased the mRNA levels of the Aβ-degrading MMPs *Mmp2* (Roher et al., 1994), *Mmp9* (P. Yan et al., 2006), and *Mmp14* (Liao and Van Nostrand, 2010) (Fig. 2B). We also found that the expression levels of *Timp3* and *Timp4* mRNAs, which encode TIMP3 and TIMP4, respectively, were decreased by AH7614 treatment (Fig. 2C). In contrast, the expression of *Bsg*, encoding extracellular MMP inducer, was decreased (Agrawal and Yong, 2011) (Fig. 2B). These data suggested that AH7614 regulated the expression of a variety of genes in astrocytes. Among them, we focused on the activities of MMPs, which are Aβ-degrading enzymes that demonstrated increased activity by AH7614 treatment. Supporting this notion, GM6001, a broad-spectrum MMP inhibitor, abolished the Aβ-degrading activity induced by AH7614 without affecting the cell viability (Fig. 3A–C). Then, we analyzed the effects of the knockdown of GPR120 in astrocytes by a recombinant lentivirus expressing shRNA targeting *Ffar4*, which encodes GPR120 (Fig. 3D). We confirmed that Aβ-degrading activity in primary astrocytes was significantly increased by *Ffar4* knockdown without any cell toxicity, and this activity was inhibited by GM6001 treatment (Fig. 3E–G). Thus, GPR120 signaling negatively controlled the Aβ-degrading activity of MMP family proteins in astrocytes.

Among the Aβ-degrading MMPs, MMP2 and MMP9 are secreted MMPs, whereas MMP14/MT1-MMP is a membrane-tethered protease (Beroun et al., 2019; Rivera et al., 2019). MMP2 and MMP9 have similar substrate preferences to gelatinases. MMP14 is known as collagenase and activates MMP2 by cleaving the prodomain of MMP2 on the cell surface. Moreover, TIMP3 is an effective inhibitor of MMP14, suggesting the complexity and redundant nature of MMPs. To clarify which MMP activity is crucial for GPR120-regulated Aβ-degrading activity, we analyzed Aβ degradation by primary astrocytes infected with a recombinant lentivirus expressing shRNA against each MMP. We found that knockdown of neither *Mmp2* (Fig. 4A–C,J) nor *Mmp9* (Fig. 4D–F,K) affected AH7614-induced Aβ degradation. In contrast, *Mmp14* RNAi abolished the effects of AH7614 without any cell toxicity (Fig. 4G–I,L). These results indicated that the inhibition of GPR120 signaling upregulated the MMP14-dependent Aβ-degrading activity.

We further analyzed the expression profiles of *FFAR4*, *MMP2*, *MMP9*, *MMP14*, *TIMP3*, and *TIMP4* mRNAs in AD brains using two public RNAseq datasets deposited in the accelerating medicines partnership-Alzheimer's disease (AMP-AD)

knowledge portal, namely, the Mayo RNAseq (MayoRNAseq) and MSBB AD cohorts (Allen et al., 2016; Wang et al., 2018). In the Mayo sample set, we found that the levels of *TIMP3*, *MMP9*, and *MMP14* mRNA were increased in the temporal cortex of AD patients (Table 3). In contrast, *FFAR4* mRNA level was significantly decreased. Consistent with this, in the analysis of the MSBB, we confirmed the increased expression level of *MMP14*, whereas the level of *FFAR4* mRNA was significantly decreased in Brodmann area 36 of AD patients, including in the parahippocampal gyrus (Fig. 5A). Furthermore, we found that *FFAR4* mRNA levels negatively correlated with *MMP14* mRNA levels (Fig. 5B). Collectively, these data strengthen our findings that the downregulation of GPR120 signaling in astrocytes is associated with the increased expression of Aβ-degrading MMP proteins, and thus with its involvement in AD pathology.

Intracerebral injection of GPR120-selective antagonist upregulated Aβ-degrading activity by MMP in AD model mice

As the brain contains high concentrations of ω3 PUFAs, GPR120 signaling is expected to be constitutively activated in the brain. The *in vitro* experiments described above prompted us to investigate whether the inhibition of GPR120 *in vivo* effectively reduces brain Aβ levels. To test this, AH7614 was injected into the right hippocampus of 12- to 15-month-old APP/PS1 mice, which coexpress mutant APP and presenilin 1 (Jankowsky et al., 2004) (Fig. 6A). Aβ deposition in these mice starts from ~6 months old and reaches a plateau at 12 months old (Minkeviciene et al., 2008; Jackson et al., 2013). Twenty-four hours after injection, hippocampi were fractionated into the TBS-soluble fraction, Triton X-100-soluble fraction, SDS-soluble fraction, and SDS-insoluble fraction. Then, the Aβ level in each fraction was analyzed. TBS-soluble Aβ levels in AH7614-injected hippocampi were significantly decreased by ~30% (Fig. 6B,C). The Triton X-100-soluble fraction contained no detectable Aβ. Aβ levels in the SDS-soluble fraction and SDS-insoluble fraction were unchanged by AH7614 injection (Fig. 6D,E). In addition, AH7614 injection showed no effects on the protein levels of APP, BACE1, sAPPβ, and C99, indicating that the Aβ production machinery was not altered by the inhibition of GPR120 signaling (Fig. 6F). Moreover, the coinjection of GM6001 with AH7614 abolished the induced Aβ degradation in the APP/PS1 mouse brain in a similar manner to that observed in primary astrocytes (Fig. 6G). These results indicated that the inhibition of GPR120 signaling in the brains of APP/PS1 mice upregulates the MMP-mediated degradation of soluble Aβ.

Discussion

In this study, we found that inhibition of GPR120 signaling in astrocytes increased Aβ degradation by MMP proteins (Fig. 7). Both antagonist treatment and RNAi experiments augmented Aβ-degrading activity, which was sensitive to the pan-MMP inhibitor GM6001. Importantly, knockdown of *Mmp14*, which is an Aβ-degrading protease and activator of other MMPs, abolished the AH7614-induced Aβ degradation. Moreover, expression levels of *MMP14* and *FFAR4*, the latter encoding GPR120, were negatively correlated in the human brain. Finally, we demonstrated that the inhibition of GPR120 signaling in the brains of AD model mice significantly reduced Aβ levels, suggesting that GPR120 signaling functionally regulates MMP-mediated proteolytic activities against Aβ *in vivo*.
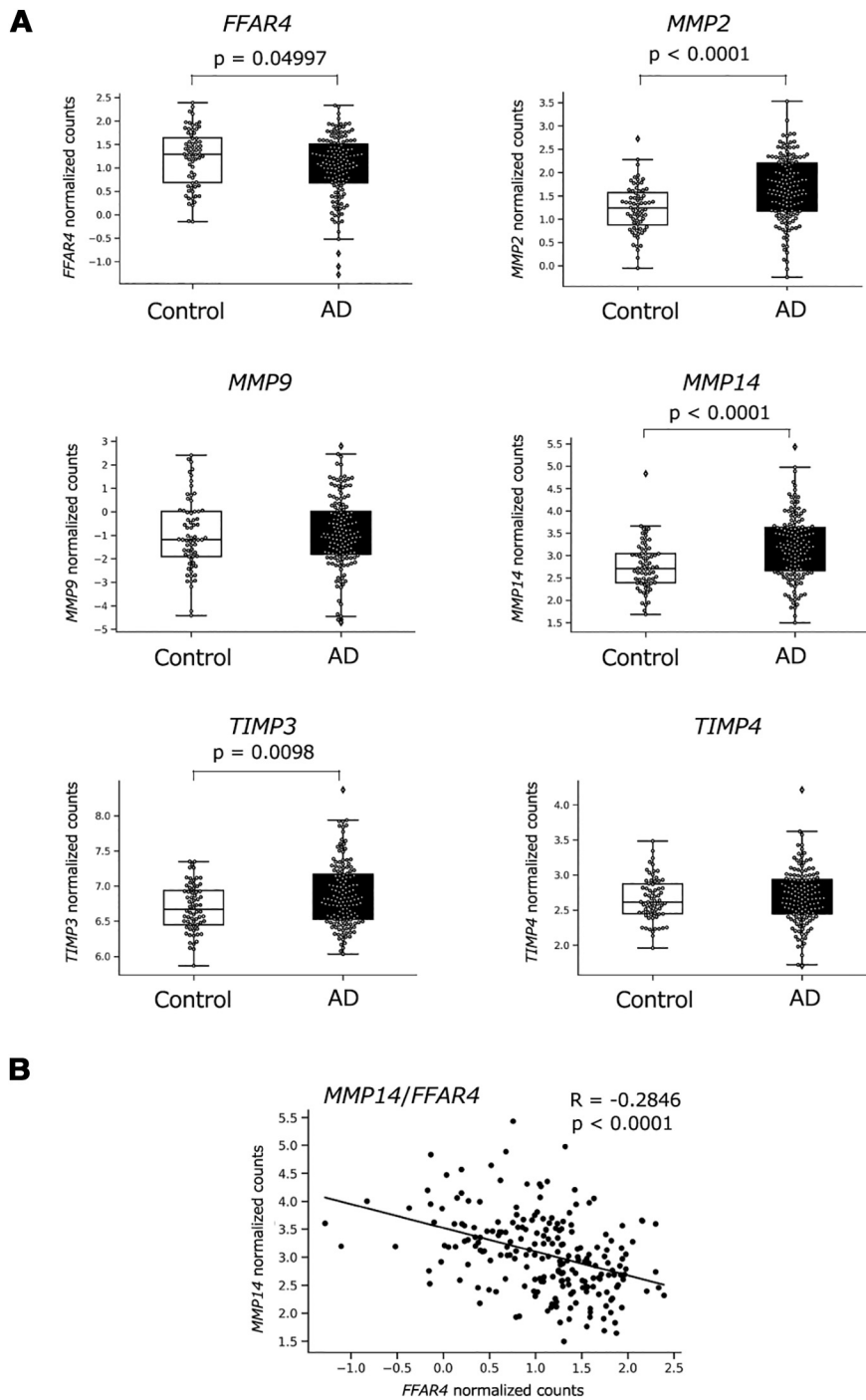
A

B

Figure 5. Changes in the expression levels of *FFAR4*, *MMP2*, *MMP9*, *MMP14*, *TIMP3*, and *TIMP4* in AD patients. **A**, Healthy control subjects (Control) were defined as those in whom neuropathology measured by CERAD was equal to 1 (*n* = 64). AD patients were the other subjects in whom neuropathology ranged from 2 to 4 (*n* = 137). *FFAR4* mRNA levels were significantly decreased in AD patients. On the other hand, *MMP2*, *MMP14*, and *TIMP3* mRNA levels were significantly increased in AD patients. *p* values were calculated by the Mann–Whitney *U* test. **B**, *FFAR4* mRNA levels negatively correlated with *MMP14* mRNA levels from 201 subjects. Line indicates the regression line. The correlation coefficient and *p* value were assessed from the Kendall rank correlation coefficient.

In peripheral organs, including adipose tissue, GPR120 is the functional receptor for *ω*3 PUFAs, leading to robust anti-inflammatory and insulin-sensitizing effects (Oh and Olefsky, 2016). Genetic ablation of the *Ffar4* gene led to obesity in mice, and genetic variants of the *FFAR4* gene have been identified in subjects with obesity and diabetes (Ichimura et al., 2012). However, the role of GPR120 in the brain remains unclear, although

several types of brain cells have been shown to express *Ffar4* mRNA (Ren et al., 2019). Our study shows that GPR120-mediated signaling in astrocytes negatively regulates proteolytic activities by regulation of the expression of several MMPs and TIMPs. As *ω*3 PUFAs are enriched in the brain, these proteolytic activities in astrocytes are thought to be constitutively suppressed in the brain. Intriguingly, several reports suggest that, in peripheral tissues, increased level of *ω*3 PUFAs suppress the expression and activity of MMPs, which are involved in the remodeling of extracellular matrices (Taguchi et al., 2014; Yun et al., 2016; Zhang et al., 2016). Thus, the constitutive inhibition of MMP activities via GPR120 signaling maintains the microenvironment of the brain (Beroun et al., 2019; Rivera et al., 2019). However, under pathologic conditions, decreased level of *ω*3 PUFAs might initiate the structural and functional remodeling of the brain microenvironment by the upregulation of MMP activities in astrocytes.

MMP2, MMP9, and MMP14 are known as Aβ-degrading proteases (Roher et al., 1994; P. Yan et al., 2006; Liao and Van Nostrand, 2010). Knockdown experiments demonstrated that MMP14 is a crucial enzyme for the AH7614-induced degradation of Aβ, although AH7614 treatment altered the expression of multiple MMP-associated genes, including *Mmp14*, *Mmp2*, *Mmp9*, *Timp3*, and *Timp4* in primary astrocytes. The molecular mechanism by which GPR120 signaling controls the expression of multiple MMPs and TIMPs remains unclear. Bsg pathway has been known to induce the expression of MMPs (Agrawal and Yong, 2011), while the inhibition of GPR120 signaling decreased the *Bsg* level in this study (Fig. 2B). Of note, The opposite expression control of MMPs and TIMPs by NF-κB has been reported in tumor metastasis and fibrosis models (Yun et al., 2016). Supporting this notion, GPR120 regulates inflammatory responses in various cells via the NF-κB pathway (Oh and Olefsky, 2016; Han et al., 2017). Thus, AH7614 appears to induce proinflammatory responses in astrocytes to augment MMP activities. As MMP14 activates MMP2 and MMP13, the latter further cleaving the pro-domain of MMP9, MMP14 is a key enzyme in GPR120-regulated Aβ degradation.

Expression analysis of human brain samples further strengthened our observation *in vitro*; that is, the expression levels of *MMP14* negatively correlated with *FFAR4* mRNA levels, supporting our notion that GPR120 signaling regulates MMP14 expression in the human brain. However, unexpectedly, we found that the expression levels of *FFAR4* mRNA were
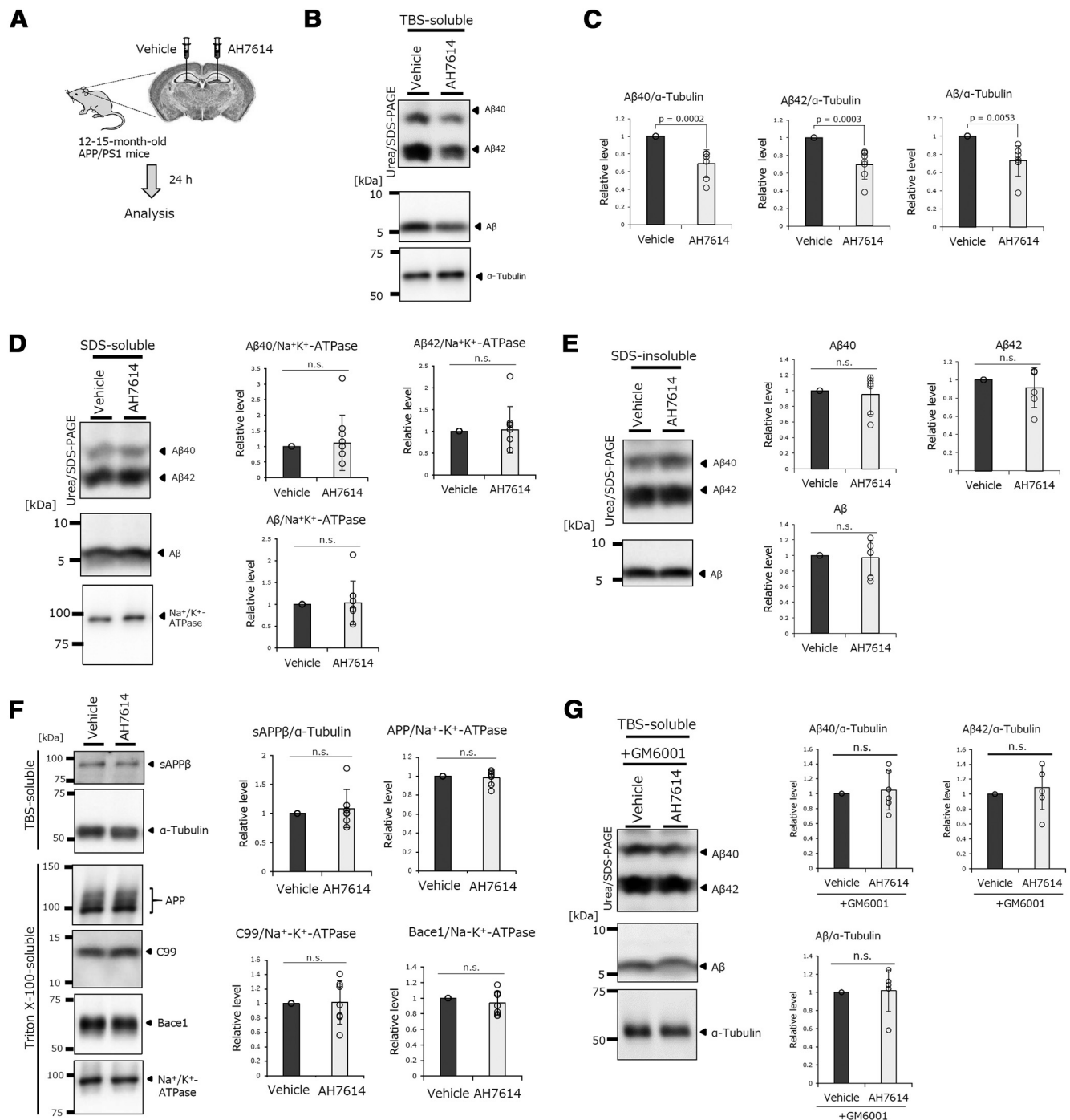
Figure 6.   Administration of AH7614 reduced soluble Aβ levels in APP/PS1 mice. ***A***, A schematic representation of the *in vivo* injection experiments. AH7614 (100 μM) was injected into the right hippocampus, and vehicle was injected into the left hippocampus of 12- to 15-month-old APP/PS1 mice. Twenty-four hours after the injection, hippocampi were collected and analyzed after sequential fractionation. ***B***, A representative Western blot of Aβ40, Aβ42, total Aβ, and α-tubulin levels in the TBS-soluble fraction of hippocampi injected with or without AH7614. ***C***, Quantified results of ***B*** (*n* = 7, mean ± SD, paired *t* test). ***D***, A representative Western blot and quantified results of Aβ40, Aβ42, total Aβ, and α-tubulin levels in SDS-soluble fractions of hippocampi injected with or without AH7614 (*n* = 7, mean ± SD, paired *t* test). ***E***, A representative Western blot and quantified results of Aβ40, Aβ42, total Aβ, and α-tubulin levels in SDS-insoluble fractions of hippocampi injected with or without AH7614 (*n* = 6, mean ± SD, paired *t* test). ***F***, Expression levels of sAPPβ, α-tubulin (TBS-soluble fraction), APP, C99, Bace1, and Na$^+$/K$^+$-ATPase (Triton X-100-soluble fractions) in fractionated hippocampi injected with or without AH7614 analyzed by Western blotting (*n* = 7, mean ± SD, paired *t* test). ***G***, A representative Western blot and quantified results of Aβ40, Aβ42, total Aβ, and α-tubulin levels in TBS-soluble fractions of hippocampi injected with or without AH7614 together with 50 μM GM6001 (*n* = 6, mean ± SD, paired *t* test).

significantly decreased in the brains of AD patients. Then, why do these patients develop AD pathology, including Aβ deposition? The most prominent difference in MMP/TIMP expression profiles was the increased expression of *TIMP3* in AD brains, whereas AH7614-treated astrocytes showed reduced *Timp3*

mRNA levels. One possible explanation of this difference is the regulation by other molecules independent of GPR120 signaling pathway, such as transcriptional factor Sp1. Some reports suggested that Sp1 activated the *Timp3* expression (Qureshi et al., 2005; D. Yan et al., 2013), and the expression level of Sp1 was
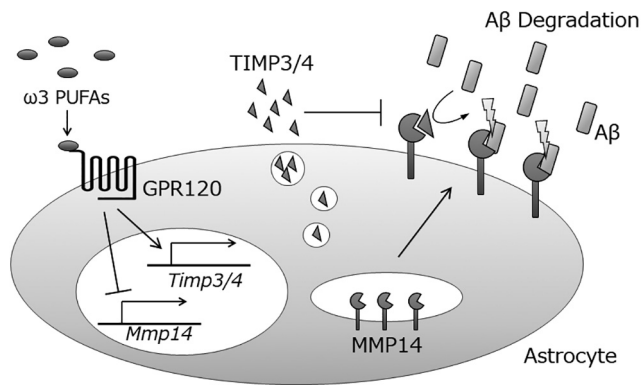
Figure 7. GPR120 signaling negatively regulates the Aβ-degrading activity in the astrocytes. Astrocytic GPR120 signaling suppressed the Aβ-degrading activity by regulating the expression levels of MMP14 and TIMP3/TIMP4.

increased in AD brain (Citron et al., 2008). Moreover, the pathologic effects of neurodegeneration in the AD brain, as well as cell-type differences, might affect the expression of MMP-associated genes, including *TIMP3*, as *FFAR4* expression was observed in multiple cells in the brain (Ren et al., 2019). Nevertheless, further genetic analyses together with single-cell technology are required for the precise understanding of the importance of GPR120 signaling in the regulation of MMPs and TIMPs in the AD brain.

Finally, we determined the possibility of GPR120 as a therapeutic target via an anti-Aβ approach using the APP/PS1 mouse model, in which the expression level of *Ffar4* mRNA is maintained after the development of Aβ plaques. The pharmacological inhibition of GPR120 signaling by the injection of AH7614 reduced the levels of soluble Aβ by 30% without affecting the expression of APP, BACE1, and γ-secretases (Fig. 6). However, the global inhibition of GPR120 is known to lead to obesity (Ichimura et al., 2012), and a GPR120-selective agonist was shown to improve insulin resistance (Oh et al., 2014). Intriguingly, GPR120 mediates multiple signaling pathways via distinct molecular mechanisms (Oh and Olefsky, 2016; Milligan et al., 2017). Metabolic control by GPR120-mediated incretin release was dependent on the Gq/G11 G-protein family and increased levels of intracellular calcium ions (Hirasawa et al., 2005). GPR120 also initiates the β-arrestin-mediated anti-inflammatory signals to attenuate NF-κB activation in immune cells (Watson et al., 2012; Han et al., 2017), the latter being involved in the expression of MMPs and TIMPs, suggesting the heterogeneity of GPR120 signaling in a cell- and/or context-dependent manner. Thus, further investigation of the signaling mechanism by which GPR120 inhibition in astrocytes increases Aβ-degrading activity at the molecular level would provide a novel therapeutic target for AD. Collectively, these results indicate that the inhibition of GPR120 signaling strongly affects Aβ economy in the brain. Our results also highlight the potential of therapeutic/preventive approaches against AD by targeting astrocytes.

References

Agrawal SM, Yong VW (2011) The many faces of EMMPRIN: roles in neuroinflammation. Biochim Biophys Acta 1812:213–219.

Allen M, Carrasquillo MM, Funk C, Heavner BD, Zou F, Younkin CS, Burgess JD, Chai HS, Crook J, Eddy JA, Li H, Logsdon B, Peters MA, Dang KK, Wang X, Serie D, Wang C, Nguyen T, Lincoln S, Malphrus K, et al. (2016) Human whole genome genotype and transcriptome data for Alzheimer's and other neurodegenerative diseases. Sci Data 3:160089.

Bazinet RP, Layé S (2014) Polyunsaturated fatty acids and their metabolites in brain function and disease. Nat Rev Neurosci 15:771–785.

Beroun A, Mitra S, Michaluk P, Pijet B, Stefaniuk M, Kaczmarek L (2019) MMPs in learning and memory and neuropsychiatric disorders. Cell Mol Life Sci 76:3207–3228.

Chiu YW, Hori Y, Ebinuma I, Sato H, Hara N, Ikeuchi T, Tomita T (2020) Identification of calcium and integrin-binding protein 1 as a novel regulator of production of amyloid β peptide using CRISPR/Cas9-based screening system. FASEB J 34:7661–7674.

Citron BA, Dennis JS, Zeitlin RS, Echeverria V (2008) Transcription factor Sp1 dysregulation in Alzheimer's disease. J Neurosci Res 86:2499–2504.

Das M, Das S (2019) Docosahexaenoic acid (DHA) induced morphological differentiation of astrocytes is associated with transcriptional upregulation and endocytosis of β2-AR. Mol Neurobiol 56:2685–2702.

Dragano NR, Solon C, Ramalho AF, de Moura RF, Razolli DS, Christiansen E, Azevedo C, Ulven T, Velloso LA (2017) Polyunsaturated fatty acid receptors, GPR40 and GPR120, are expressed in the hypothalamus and control energy homeostasis and inflammation. J Neuroinflammation 14:91.

Florent S, Malaplate-Armand C, Youssef I, Kriem B, Koziel V, Escanyé MC, Fifre A, Sponne I, Leininger-Muller B, Olivier JL, Pillot T, Oster T (2006) Docosahexaenoic acid prevents neuronal apoptosis induced by soluble amyloid-β oligomers. J Neurochem 96:385–395.

Fukumoto H, Tomita T, Matsunaga H, Ishibashi Y, Saido TC, Iwatsubo T (1999) Primary cultures of neuronal and non-neuronal rat brain cells secrete similar proportions of amyloid β peptides ending at Aβ40 and Aβ42. Neuroreport 10:2965–2969.

Gotoh C, Hong YH, Iga T, Hishikawa D, Suzuki Y, Song SH, Choi KC, Adachi T, Hirasawa A, Tsujimoto G, Sasaki S, Roh SG (2007) The regulation of adipogenesis through GPR120. Biochem Biophys Res Commun 354:591–597.

Hamazaki H (1996) Cathepsin D is involved in the clearance of Alzheimer's β-amyloid protein. FEBS Lett 396:139–142.

Han L, Song S, Niu Y, Meng M, Wang C (2017) Eicosapentaenoic acid (EPA) induced macrophages activation through GPR120-mediated Raf-ERK1/2-IKKβ-NF-κB p65 signaling pathways. Nutrients 9:937.

Heras-Sandoval D, Pedraza-Chaverri J, Pérez-Rojas JM (2016) Role of docosahexaenoic acid in the modulation of glial cells in Alzheimer's disease. J Neuroinflammation 13:61.

Hilgendorf KI, Johnson CT, Mezger A, Rice SL, Norris AM, Demeter J, Greenleaf WJ, Reiter JF, Kopinke D, Jackson PK (2019) Omega-3 fatty acids activate ciliary FFAR4 to control adipogenesis. Cell 179:1289–1305. e21.

Hirasawa A, Tsumaya K, Awaji T, Katsuma S, Adachi T, Yamada M, Sugimoto Y, Miyazaki S, Tsujimoto G (2005) Free fatty acids regulate gut incretin glucagon-like peptide-1 secretion through GPR120. Nat Med 11:90–94.

Hori Y, Hashimoto T, Nomoto H, Hyman BT, Iwatsubo T (2015) Role of apolipoprotein E in β-amyloidogenesis: isoform-specific effects on protofibril to fibril conversion of aβ in vitro and brain aβ deposition in vivo. J Biol Chem 290:15163–15174.

Hu J, Igarashi A, Kamata M, Nakagawa H (2001) Angiotensin-converting enzyme degrades Alzheimer amyloid β-peptide (Aβ); retards Aβ aggregation, deposition, fibril formation; and inhibits cytotoxicity. J Biol Chem 276:47863–47868.

Ichimura A, Hirasawa A, Poulain-Godefroy O, Bonnefond A, Hara T, Yengo L, Kimura I, Leloire A, Liu N, Iida K, Choquet H, Besnard P, Lecoeur C, Vivequin S, Ayukawa K, Takeuchi M, Ozawa K, Tauber M, Maffeis C, Morandi A, et al. (2012) Dysfunction of lipid sensor GPR120 leads to obesity in both mouse and human. Nature 483:350–354.

Ishihara T, Yoshida M, Arita M (2019) Omega-3 fatty acid-derived mediators that control inflammation and tissue homeostasis. Int Immunol 31:559–567.

Jackson HM, Soto I, Graham LC, Carter GW, Howell GR (2013) Clustering of transcriptional profiles identifies changes to insulin signaling as an early event in a mouse model of Alzheimer's disease. BMC Genomics 14:831–812.

Jankowsky JL, Fadale DJ, Anderson J, Xu GM, Gonzales V, Jenkins NA, Copeland NG, Lee MK, Younkin LH, Wagner SL, Younkin SG, Borchelt DR (2004) Mutant presenilins specifically elevate the levels of the 42 residue β-amyloid peptide in vivo: evidence for augmentation of a 42-specific γ secretase. Hum Mol Genet 13:159–170.

Jonsson T, Atwal JK, Steinberg S, Snaedal J, Jonsson PV, Bjornsson S, Stefansson H, Sulem P, Gudbjartsson D, Maloney J, Hoyte K, Gustafson A, Liu Y, Lu Y, Bhangale T, Graham RR, Huttenlocher J, Bjornsdottir G, Andreassen OA, Jönsson EG, et al. (2012) A mutation in APP protects against Alzheimer's disease and age-related cognitive decline. Nature 488:96–99.

Kidana K, Tatebe T, Ito K, Hara N, Kakita A, Saito T, Takatori S, Ouchi Y, Ikeuchi T, Makino M, Saido TC, Akishita M, Iwatsubo T, Hori Y, Tomita T (2018) Loss of kallikrein-related peptidase 7 exacerbates amyloid pathology in Alzheimer's disease model mice. EMBO Mol Med 10:e8184.

Kikuchi K, Kidana K, Tatebe T, Tomita T (2017) Dysregulated metabolism of the amyloid-β protein and therapeutic approaches in Alzheimer disease. J Cell Biochem 118:4183–4190.

Kim HY, Akbar M, Kim YS (2010) Phosphatidylserine-dependent neuroprotective signaling promoted by docosahexaenoic acid. Prostaglandins Leukot Essent Fatty Acids 82:165–172.

Lewis DL, Hagstrom JE, Loomis AG, Wolff JA, Herweijer H (2002) Efficient delivery of siRNA for inhibition of gene expression in postnatal mice. Nat Genet 32:107–108.

Liao MC, Van Nostrand WE (2010) Degradation of soluble and fibrillar amyloid β-protein by matrix metalloproteinase (MT1-MMP) in vitro. Biochemistry 49:1127–1136.

Liao MC, Ahmed M, Smith SO, Van Nostrand WE (2009) Degradation of amyloid β protein by purified myelin basic protein. J Biol Chem 284:28917–28925.

Liu JJ, Green P, Mann JJ, Rapoport SI, Sublette ME (2015) Pathways of polyunsaturated fatty acid utilization: implications for brain function in neuropsychiatric health and disease. Brain Res 1597:220–246.

Mawuenyega KG, Sigurdson W, Ovod V, Munsell L, Kasten T, Morris JC, Yarasheski KE, Bateman RJ (2010) Decreased clearance of CNS β-amyloid in Alzheimer's disease. Science 330:1774.

McDermott JR, Gibson AM (1996) Degradation of Alzheimer's beta-amyloid protein by human cathepsin D. Neuroreport 7:2163–2166.

Milligan G, Alvarez-Curto E, Hudson BD, Prihandoko R, Tobin AB (2017) FFA4/GPR120: pharmacology and therapeutic opportunities. Trends Pharmacol Sci 38:809–821.

Minkeviciene R, Ihalainen J, Malm T, Matilainen O, Keksa-Goldsteine V, Goldsteins G, Iivonen H, Leguit N, Glennon J, Koistinaho J, Banerjee P, Tanila H (2008) Age-related decrease in stimulated glutamate release and vesicular glutamate transporters in APP/PS1 transgenic and wild-type mice. J Neurochem 105:584–594.

Miyagawa T, Ebinuma I, Morohashi Y, Hori Y, Young Chang M, Hattori H, Maehara T, Yokoshima S, Fukuyama T, Tsuji S, Iwatsubo T, Prendergast GC, Tomita T (2016) BIN1 regulates BACE1 intracellular trafficking and amyloid-β production. Hum Mol Genet 25:ddw146.

Morris MC, Evans DA, Bienias JL, Tangney CC, Bennett DA, Wilson RS, Aggarwal N, Schneider J (2003) Consumption of fish and n-3 fatty acids and risk of incident Alzheimer disease. Arch Neurol 60:940–946.

O'Brien JS, Sampson EL (1965) Lipid composition of the normal human brain: gray matter, white matter, and myelin. J Lipid Res 6:537–544.

Oh DY, Olefsky JM (2016) G protein-coupled receptors as targets for anti-diabetic therapeutics. Nat Rev Drug Discov 15:161–172.

Oh DY, Talukdar S, Bae EJ, Imamura T, Morinaga H, Fan W, Li P, Lu WJ, Watkins SM, Olefsky JM (2010) GPR120 is an omega-3 fatty acid receptor mediating potent anti-inflammatory and insulin-sensitizing effects. Cell 142:687–698.

Oh DY, Walenta E, Akiyama TE, Lagakos WS, Lackey D, Pessentheiner AR, Sasik R, Hah N, Chi TJ, Cox JM, Powels MA, Di Salvo J, Sinz C, Watkins SM, Armando AM, Chung H, Evans RM, Quehenberger O, McNelis J, Bogner-Strauss JG, et al. (2014) A Gpr120-selective agonist improves insulin resistance and chronic inflammation in obese mice. Nat Med 20:942–947.

Ohki Y, Higo T, Uemura K, Shimada N, Osawa S, Berezovska O, Yokoshima S, Fukuyama T, Tomita T, Iwatsubo T (2011) Phenylpiperidine-type γ-secretase modulators target the transmembrane domain 1 of presenilin 1. EMBO J 30:4815–4824.

Okuno H, Akashi K, Ishii Y, Yagishita-Kyo N, Suzuki K, Nonaka M, Kawashima T, Fujii H, Takemoto-Kimura S, Abe M, Natsume R, Chowdhury S, Sakimura K, Worley PF, Bito H (2012) Inverse synaptic tagging of inactive synapses via dynamic interaction of Arc/Arg3.1 with CaMKIIβ. Cell 149:886–898.

Podlisny MB, Ostaszewski BL, Squazzo SL, Koo EH, Rydell RE, Teplow DB, Selkoe DJ (1995) Aggregation of secreted amyloid β-protein into sodium dodecyl sulfate-stable oligomers in cell culture. J Biol Chem 270:9564–9570.

Qi-Takahara Y, Morishima-Kawashima M, Tanimura Y, Dolios G, Hirotani N, Horikoshi Y, Kametani F, Maeda M, Saido TC, Wang R, Ihara Y (2005) Longer forms of amyloid β protein: implications for the mechanism of intramembrane cleavage by γ-secretase. J Neurosci 25:436–445.

Qiu WQ, Walsh DM, Ye Z, Vekrellis K, Zhang J, Podlisny MB, Rosner MR, Safavi A, Hersh LB, Selkoe DJ (1998) Insulin-degrading enzyme regulates extracellular levels of amyloid β-protein by degradation. J Biol Chem 273:32730–32738.

Qureshi HY, Sylvester J, El Mabrouk M, Zafarullah M (2005) TGF-β-induced expression of tissue inhibitor of metalloproteinases-3 gene in chondrocytes is mediated by extracellular signal-regulated kinase pathway and Sp1 transcription factor. J Cell Physiol 203:345–352.

Ren Z, Chen L, Wang Y, Wei X, Zeng S, Zheng Y, Gao C, Liu H (2019) Activation of the omega-3 fatty acid receptor GPR120 protects against focal cerebral ischemic injury by preventing inflammation and apoptosis in mice. J Immunol 202:747–759.

Ries M, Sastre M (2016) Mechanisms of Aβ clearance and degradation by glial cells. Front Aging Neurosci 8:1–9.

Rivera S, García-González L, Khrestchatisky M, Baranger K (2019) Metalloproteinases and their tissue inhibitors in Alzheimer's disease and other neurodegenerative disorders. Cell Mol Life Sci 76:3167–3191.

Roher AE, Kasunic TC, Woods AS, Cotter RJ, Ball MJ, Fridman R (1994) Proteolysis of Aβ peptide from Alzheimer disease brain by gelatinase A. Biochem Biophys Res Commun 205:1755–1761.

Saido T, Leissring MA (2012) Proteolytic degradation of amyloid β-protein. Cold Spring Harb Perspect Med 2:a006379. PMC]

Schwab JM, Chiang N, Arita M, Serhan CN (2007) Resolvin E1 and protectin D1 activate inflammation-resolution programmes. Nature 447:869–874.

Shirotani K, Tsubuki S, Iwata N, Takaki Y, Harigaya W, Maruyama K, Kiryu-Seo S, Kiyama H, Iwata H, Tomita T, Iwatsubo T, Saido TC (2001) Neprilysin degrades both amyloid β peptides 1-40 and 1-42 most rapidly and efficiently among thiorphan- and phosphoramidon-sensitive endopeptidases. J Biol Chem 276:21895–21901.

Sparks SM, Chen G, Collins JL, Danger D, Dock ST, Jayawickreme C, Jenkinson S, Laudeman C, Leesnitzer MA, Liang X, Maloney P, McCoy DC, Moncol D, Rash V, Rimele T, Vulimiri P, Way JM, Ross S (2014) Identification of diarylsulfonamides as agonists of the free fatty acid receptor 4 (FFA4/GPR120). Bioorg Med Chem Lett 24:3100–3103.

Stewart SA, Dykxhoorn DM, Palliser D, Mizuno H, Yu EY, An DS, Sabatini DM, Chen IS, Hahn WC, Sharp PA, Weinberg RA, Novina CD (2003) Lentivirus-delivered stable gene silencing by RNAi in primary cells. RNA 9:493–501.

Taguchi A, Kawana K, Tomio K, Yamashita A, Isobe Y, Nagasaka K, Koga K, Inoue T, Nishida H, Kojima S, Adachi K, Matsumoto Y, Arimoto T, Wada-Hiraike O, Oda K, Kang JX, Arai H, Arita M, Osuga Y, Fujii T (2014) Matrix metalloproteinase (MMP)-9 in cancer-associated fibroblasts (CAFs) is suppressed by omega-3 polyunsaturated fatty acids in vitro and in vivo. PLoS One 9:e89605.

Tomita T (2017) Aberrant proteolytic processing and therapeutic strategies in Alzheimer disease. Adv Biol Regul 64:33–38.

Tomita T, Maruyama K, Saido TC, Kume H, Shinozaki K, Tokuhiro S, Capell A, Walter J, Grünberg J, Haass C, Iwatsubo T, Obata K (1997) The presenilin 2 mutation (N141I) linked to familial Alzheimer disease (Volga German families) increases the secretion of amyloid β protein ending at the 42nd (or 43rd) residue. Proc Natl Acad Sci USA 94:2025–2030.

Van Nostrand WE, Porter M (1999) Plasmin cleavage of the amyloid β-protein: alteration of secondary structure and stimulation of tissue plasminogen activator activity. Biochemistry 38:11570–11576.

Wang M, Beckmann ND, Roussos P, Wang E, Zhou X, Wang Q, Ming C, Neff R, Ma W, Fullard JF, Hauberg ME, Bendl J, Peters MA, Logsdon B, Wang P, Mahajan M, Mangravite LM, Dammer EB, Duong DM, Lah JJ, et al. (2018) The Mount Sinai cohort of large-scale genomic, transcriptomic and proteomic data in Alzheimer's disease. Sci Data 5:1–16.

Watson SJ, Brown AJ, Holliday ND (2012) Differential signaling by splice variants of the human free fatty acid receptor GPR120. Mol Pharmacol 81:631–642.

Watterson KR, Hansen SV, Hudson BD, Alvarez-Curto E, Raihan SZ, Azevedo CM, Martin G, Dunlop J, Yarwood SJ, Ulven T, Milligan G (2017) Probe-dependent negative allosteric modulators of the long-chain free fatty acid receptor FFA4. Mol Pharmacol 91:630–641.

Yamin R, Bagchi S, Hildebrant R, Scaloni A, Widom RL, Abraham CR (2007) Acyl peptide hydrolase, a serine proteinase isolated from conditioned medium of neuroblastoma cells, degrades the amyloid-β peptide. J Neurochem 100:458–467.

Yan D, Chen D, Hawse JR, van Wijnen AJ, Im HJ (2013) Bovine lactoferricin induces TIMP-3 via the ERK1/2-Sp1 axis in human articular chondrocytes. Gene 517:12–18.

Yan P, Hu X, Song H, Yin K, Bateman RJ, Cirrito JR, Xiao Q, Hsu FF, Turk JW, Xu J, Hsu CY, Holtzman DM, Lee JM (2006) Matrix metalloproteinase-9 degrades amyloid-β fibrils in vitro and compact plaques in situ. J Biol Chem 281:24566–24574.

Yu JZ, Wang J, Sheridan SD, Perlis RH, Rasenick MM (2020) N-3 polyunsaturated fatty acids promote astrocyte differentiation and neurotrophin production independent of cAMP in patient-derived neural stem cells. Mol Psychiatry Advance online publication. Retrieved Jun 5, 2020. doi: 10.1038/s41380-020-0786-5.

Yun EJ, Song KS, Shin S, Kim S, Heo JY, Kweon GR, Wu T, Park JI, Lim K (2016) Docosahexaenoic acid suppresses breast cancer cell metastasis by targeting matrix-metalloproteinases. Oncotarget 7:49961–49971.

Zhang W, Zhang H, Mu H, Zhu W, Jiang X, Hu X, Shi Y, Leak RK, Dong Q, Chen J, Gao Y (2016) Omega-3 polyunsaturated fatty acids mitigate blood–brain barrier disruption after hypoxic-ischemic brain injury. Neurobiol Dis 91:37–46.

Zhao Y, Calon F, Julien C, Winkler JW, Petasis NA, Lukiw WJ, Bazan NG (2011) Docosahexaenoic acid-derived neuroprotectin D1 induces neuronal survival via secretase- and PPARγ-mediated mechanisms in Alzheimer's disease models. PLoS One 6:e15816.